

Study of Synthesis, Structural and electrical nature of $Ba_{0.9}Ca_{0.1}TiO_3$ ceramic material

Arpita Patel^{1#} and Rajesh Kumar Katare¹

¹Department of Physics, SAGE University, Indore, 452001, India

Abstract— $BaTiO_3$ remains a good choice lead free material because of its good dielectric characteristics, environmental friendliness, chemical stability and cost-effective synthesis. Its high relative permittivity (ϵ') and low dielectric loss make $BaTiO_3$ an excellent choice for several applications. Barium calcium titanate (Ba,Ca) TiO_3 is used in electrical material applications. Also, these materials are attracting attention as ceramic capacitors in which dielectric properties of the BT are improved. BCT solid solutions are specifically used in multilayer ceramic capacitor applications and in various other applications like: dielectric filters, antennas, resonators, duplexers and phase shifters, and piezoelectric actuator. Hereby, we focus on the BCT material to synthesize it in solid solution form using solid state route and emphasized on its structural and electrical properties. The sample has been found to crystallize into tetragonal structure (P4mm). The dielectric permittivity is found to be high with low loss tangent values. Impedance studies for frequency dependence revealed to be decreasing with increasing frequency and thereby conduction increases for in both real and imaginary cases. Nyquist's plot reveals the distribution of relaxation time and hence infers the non-Debye behaviour.

Keywords: Crystal structure; Solid State Route; Dielectric materials; ferroelectric properties; energy bandgap.

INTRODUCTION

Materials based on barium titanate, sometimes known as $BaTiO_3$ or BT, have been the subject of much research due to its intriguing electrical characteristics, which include high dielectric constant, low dielectric loss, ferroelectric, piezoelectric, and pyroelectric behavior. In the years following its discovery, BT was the dielectric ferroelectric perovskite oxide that was most frequently employed in electrical and electronic applications. Devices with positive temperature coefficients, pulse generators, infrared detectors, voltage-tunable microwave electronics, multilayer

ceramic capacitors, actuators, lead-free piezoelectric transducers, and charge storage units are just a few of the many uses for perovskite oxides derived from BT in household appliances [1,2].

Because of its high dielectric constant, polarization, and high piezoelectric capabilities, research emphasis has been focused on lead-free and ecologically acceptable dielectric $BaTiO_3$ based piezoelectric materials [3]. Energy storage capacitors can benefit from the usage of BT-based high dielectric constant materials with low dielectric loss and high dielectric breakdown field.

The ferroelectric powder doping process The intrinsic ability of the perovskite structure to host ions of varying sizes and the enormous number of various dopants that may be inserted in the titanate barium (BT) lattice make $BaTiO_3$ crucial for the production of electrical and electronic devices. $Ba_{1-x}Ca_xTiO_3$ (BCT) is formed in the tetragonal phase of $BaTiO_3$, when Ca^{2+} replaces Ba^{2+} in the compound. The ferroelectric phase exhibiting spontaneous polarization is called the tetragonal form. Because the polarization process occurred in the tetragonal form in the absence of an external electric field and allowed for electric field control, this mechanism makes BT a viable element for optoelectronic applications [5]. Barium calcium titanate's physical characteristics are improved for the creation of opto-electric materials through Ca^{2+} doping. Ca doping is essential for reducing electrical resistance, and the amount of Ca atoms in the crystal lattice is significant because it directly affects the crystal lattice's ability to predict the ferroelectric characteristics and altered electronic structure of $BaTiO_3$. Moreover, comprehending the spontaneous polarization at ambient temperature requires an understanding of the behavior of the Ca atom as a dopant in the host lattice [6].

REVIEW OF LITERATURE

BaTiO₃ is still a hot topic in material research and its property exploitation in advanced technology employing Ca as substituent is adding its technological prosperity. In this connection we have used some research works as an inspiration to carry out this project. Here we discussed in brief their achievements:

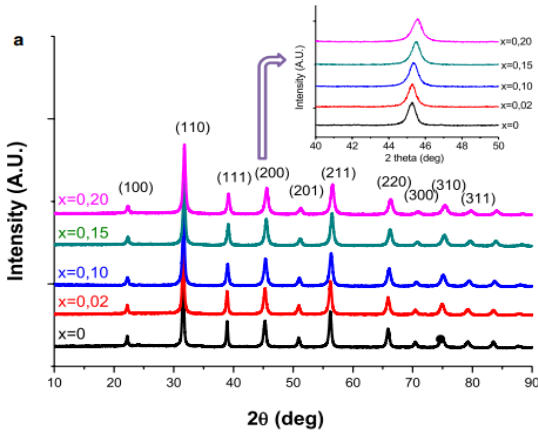


Figure 1: XRD spectra of Ba_{1-x}Ca_xTiO₃ (BCT) ceramic materials

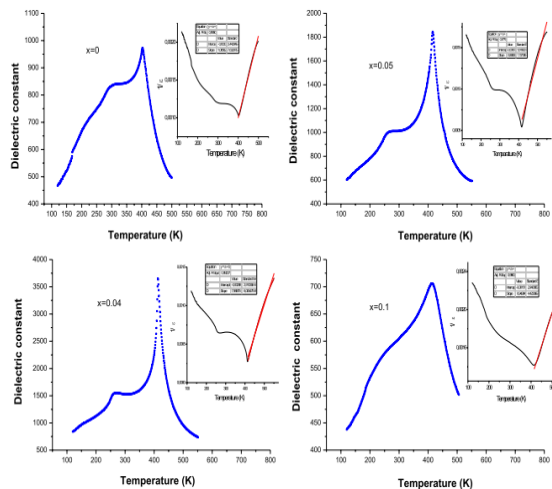


Figure 2: Temperature dependent dielectric properties of Ba_{1-x}Ca_xTiO₃ (BCT) ceramic materials

Khedri et. al reported Ba_{1-x}Ca_xTiO₃ (BCT) ceramics prepared by sol-gel process and studied their photoluminescence (PL), dielectric properties in addition to their structural properties. They witnessed that structural and dielectric properties are significantly influenced by incorporation of calcium ion in BaTiO₃ (BT). The band gap reduction was witnessed. Furthermore, Ca substitution greatly affected the grain size and Curie temperature of the Ba_{1-x}Ca_xTiO₃ ceramics [7]. The XRD patterns of

Ba_{1-x}Ca_xTiO₃ (BCT) ceramic materials is shown as Figure 1 and the temperature dependent dielectric properties are depicted by Figure 2.

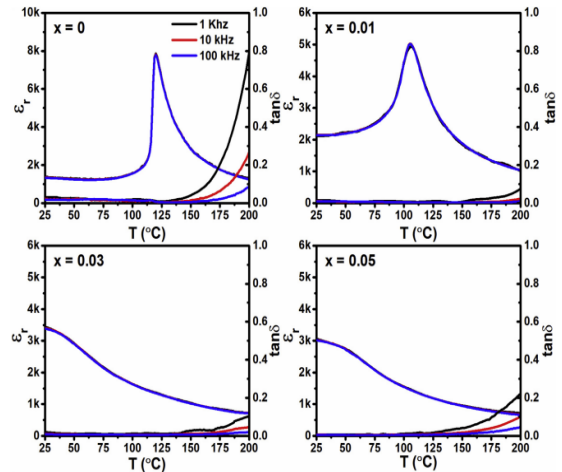


Figure 3: Temperature dependent dielectric properties of Ba_{1-x}Ca_xTiO₃ (BCT) ceramic materials

Raz et. al. reports the Ca²⁺ substituted BaTiO₃ prepared by solid state route and emphasized on its structure, dielectric, ferroelectric and optical properties. With Ca substitution, the Curie point (*T_c*) shifted to room temperature. The dielectric constant and loss value obtained are represented by Figure 3. Energy density calculated from the P-E hysteresis loops showed an increase in energy density storage efficiency with Ca-concentration and was found to be 84% for x = 0.05 sample. The optical band gap of the samples varied from 2.84 to 3.14 eV with change in x as shown by Figure 4 which was associated to the phase transition and oxygen vacancies [8].

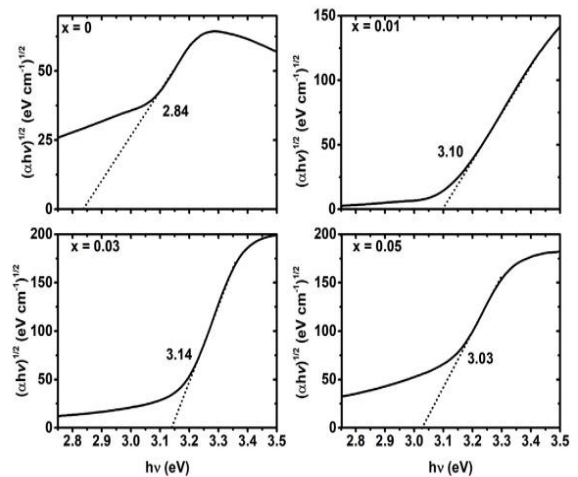


Figure 4: Temperature dependent dielectric properties of Ba_{1-x}Ca_xTiO₃ (BCT) ceramic materials

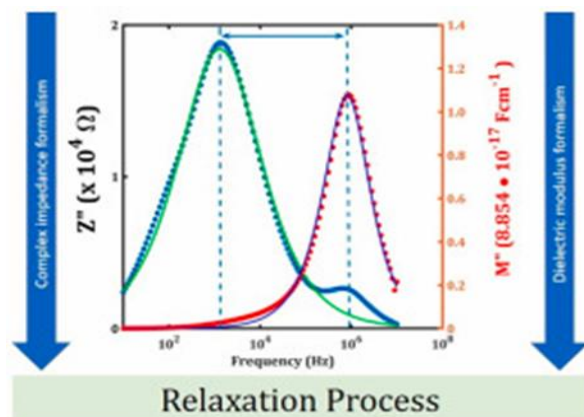


Figure 5: Impedance and electric modulus of $\text{Ba}_{1-x}\text{Ca}_x\text{TiO}_3$ (BCT) ceramic material

The dielectric modulus and complex impedance along with Relaxation processes of $\text{Ba}_{1-x}\text{Ca}_x\text{TiO}_3$ ceramics with $x = 0.05, 0.10$ and 0.23

a contents were studied. The complex impedance formalism reveals predominant time distribution relaxation function to be a Cole-Cole type, whereas dielectric modulus formalism supports non-Debye relaxation functions depicted in Figure 5. The study insists on the potential of using both impedance and dielectric modulus formalisms to identify and quantify non-Debye relaxation process and conducting properties in mixed electronic-ionic conductors [9].

Experimental Details

The $\text{Ba}_{0.9}\text{Ca}_{0.1}\text{TiO}_3$ sample was prepared by solid state reaction method. Here we used raw materials in the form of oxides and carbonated such as BaCO_3 , TiO_2 , CaCO_3 . These materials were purchased from Loba Chem. Pvt. Ltd. All these materials were used without preheating. The 5g samples were taken according to the molecular formula of the sample. After weighing the stoichiometric quantities of the sample on the sensitive digital balance, these materials were crushed using the agate-mortar pestle for 5h and then heated in Muffle furnace at 1000°C for 5h. the preparation process was repeated to as method employed is usually called the double calcination process. The final calcined powder was ground for half an hour to convert it into the fine powder. From this fine powder, pellets in the circular disc shape form were formed under hydraulic press at pressure of 5 tons per inch. For compact pellet formation, a binder (polyvinyl alcohol, PVA) was used. The pellets were sintered for 5h at 1150°C . For electrical measurements, the pellets were silver polished on it circular surface to form smooth and conducting surface

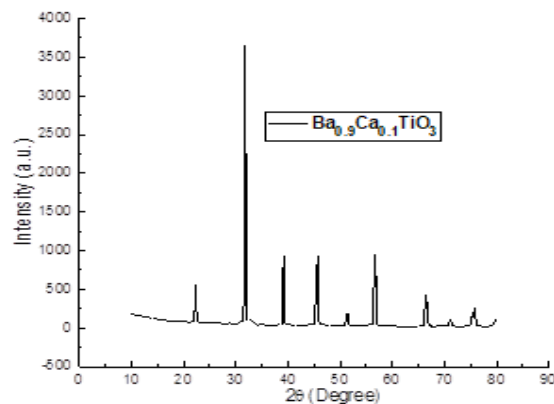


Figure 6: X-ray diffraction plot of $\text{Ba}_{0.9}\text{Ca}_{0.1}\text{TiO}_3$ perovskite compound

RESULTS AND DISCUSSION

X-ray diffraction data analysis

The chemical compound of the type $\text{Ba}_{0.9}\text{Ca}_{0.1}\text{TiO}_3$ precisely single phase in nature has been synthesized by high temperature treatment via solid state reaction method. For structural investigations, a reliable characterization known as X-ray diffraction technique has been exploited. The data was collected using Bruker D8 Advanced diffractometer with wavelength, $\lambda = 1.5406\text{\AA}$ having Cu as radiation source. The data was collected in the angular range of 10° to 90° with a step size of 0.02° . The obtained data was plotted using Origin 16 software and the spectrum was displayed as Figure 6.

The XRD data analysis has revealed that $\text{Ba}_{0.9}\text{Ca}_{0.1}\text{TiO}_3$ compound has crystallized in to the tetragonal (P4mm) crystal structure [10]. The associated phase group is P4mm. The sample is polycrystalline in nature. It possesses higher crystallinity revealed from the sharpness and higher intensity of the diffraction peaks evident from the XRD spectrum. The XRD spectrum of $\text{Ba}_{0.9}\text{Ca}_{0.1}\text{TiO}_3$ sample further reveals that the as prepared polycrystalline sample inherits higher average size of crystallites. The comment has been passed based on the narrowness of the reflections in the spectrum as it is known that low FWHM is inversely proportional to the average size of crystallites of the sample under investigations.

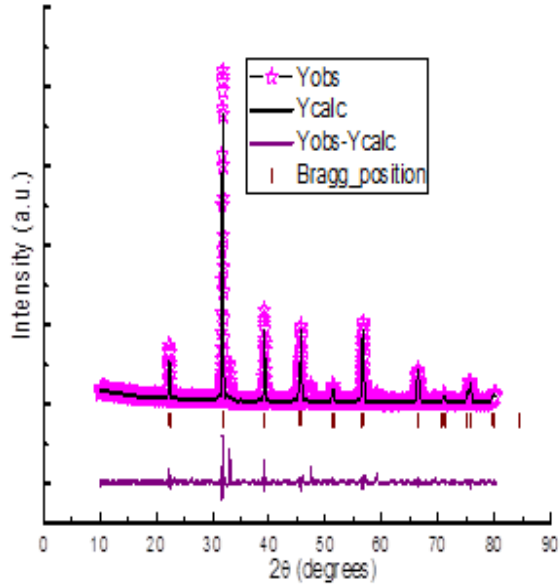


Figure 7: Rietveld refinement plot of X-ray diffraction data of Ba_{0.9}Ca_{0.1}TiO₃ perovskite compound

The average size of the crystallites of Ba_{0.9}Ca_{0.1}TiO₃ sample was calculated employing Scherer’s formula viz., $t = k\lambda / \beta \cos\theta$, where λ is wavelength of the Cu source used in the diffractometer, k is a constant known as shape factor and its value is generally taken as 0.9, β is FWHM of the characteristic reflection peaks used for the calculation of crystallite size and θ is the diffraction angle. The size of the crystallites obtained is 110nm.

The Ba_{0.9}Ca_{0.1}TiO₃ sample was also analyzed for structural properties using Rietveld refinement of the XRD data. The Figure 2 represents the Rietveld refinement of Ba_{0.9}Ca_{0.1}TiO₃ sample. All the structure related parameters obtained from the refinement are demonstrated in the Table1.

DIELECTRIC STUDIES

As illustrated in Figure 8 the dielectric constants of the Ba_{0.9}Ca_{0.1}TiO₃ sample have been tested in the frequency range of 20 Hz to 1 MHz. The dielectric constant exhibits dispersion behavior as it drops with frequency and reaches a constant value at higher frequencies. In perovskite ferroelectric materials, dielectric relaxations at lower frequencies indicate how polarization changes in response to an applied electric field that varies over time. It is frequency dependent because different polarization mechanisms work at different frequencies [11,12].

Space group	P4mm
Crystal structure	Tetragonal
a:b:c(Å)	3.9687:3.9687 :3.9952
Volume	62.9267Å ³
Density	4.307 g/cm ³
R _p , R _{wp} , R _e	32.5, 32.4, 16.4
Chi square	3.898
Goodness of fit	2.1

Grain size, orientation, and complexity all have a significant impact on the dielectric characteristics, as do ionic space-charge carriers. As a result, ionic space-charge carriers, such as oxygen vacancies and defects created during sample preparation may be connected to low-frequency dielectric relaxations. Because of space charge polarization, a large dielectric constant value is seen at lower frequencies, suggesting an uneven dielectric structure in the sample. Higher frequencies have an unchanging dielectric constant, which could be attributed to the incapacity of electric dipoles to track the rapid fluctuations in the applied alternating electric field [13].

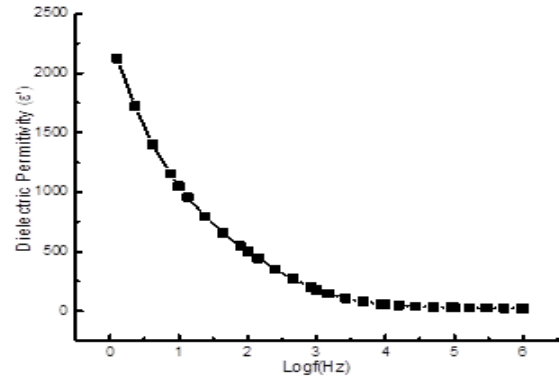


Figure 8: Dielectric permittivity plot of Ba_{0.9}Ca_{0.1}TiO₃ perovskite compound

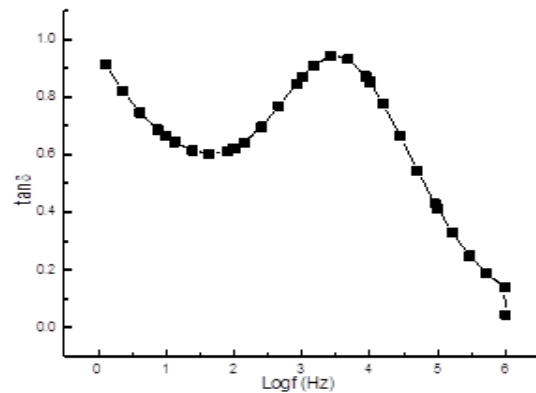


Figure 9: dielectric loss plot of Ba_{0.9}Ca_{0.1}TiO₃ perovskite compound

The energy dissipation caused by friction between dipoles is thought to be released in the form of heat produced by the dielectric medium. The formula for calculating the dielectric constant is $\epsilon = Ct / \epsilon_0 A$, where 'C' stands for capacitance, 't' for sample thickness (pellet), 'A' for the area of the pellet's polished circular surface, and ' ϵ_0 ' for free space permittivity, which is equal to 8.854×10^{-12} (F/m). Figure 9 displays the dielectric loss ($\tan\delta$) observed at room temperature. The dielectric loss graph initially exhibits a falling trend as field values increase. Following this, the dielectric loss achieves its maximum value and then behaves normally in response to the field, much like the dielectric constant of dielectric materials. The appearance of shoulder infers the resonance phenomenon where hopping frequency of the metal ions matches the frequency of the applied field. The graph shows higher values of dielectric loss at lower frequency an at the frequency values corresponding to hump peak [14-16].

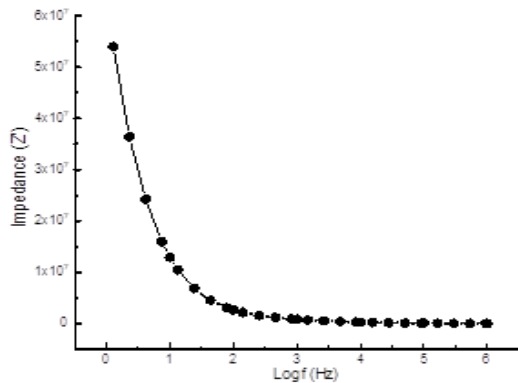


Figure 10: Impedance (real part) plot of $Ba_{0.9}Ca_{0.1}TiO_3$ perovskite compound

IMPEDANCE STUDIES

One essential method for illuminating the electrical characteristics of the material is complex impedance spectroscopy, or CIS. The genuine representation of the physical properties of the sample is distinguished by the real and imaginary components of impedance. Using this method, the AC response of a system to a sinusoidal disturbance is examined, and the impedance is then computed in relation to the frequency of the disturbance. Figure 10 shows how the real component of impedance (Z') varies with frequency. When the frequency rises above 10 kHz, the real part of the impedance monotonically declines, reaching a constant value at higher frequencies. It's possible that

the trend of merging at higher frequencies regardless of temperature is caused by the release of space charge or a continuous reduction of barrier characteristics [17].

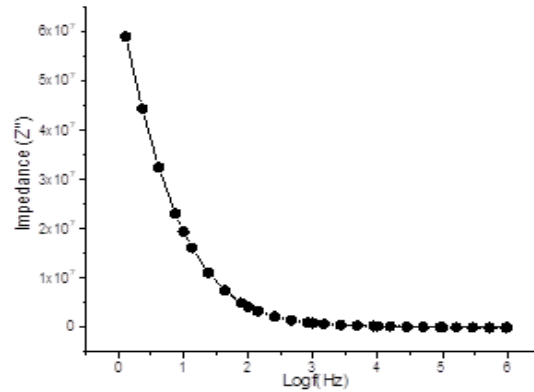


Figure 11: Impedance (Imaginary part) plot of $Ba_{0.9}Ca_{0.1}TiO_3$ perovskite compound

The frequency dependent imaginary component of impedance (Z'') is shown in Figure 11. The distribution of relaxation time is represented by the Z'' variation. At normal temperature, the major relaxation species are the electrons and immobile charges. Nonetheless, it's thought that at high temperatures, flaws or oxygen vacancies could be present. The localized site hopping of oxygen ion vacancies may give rise to electrical conductivity. [18, 19]

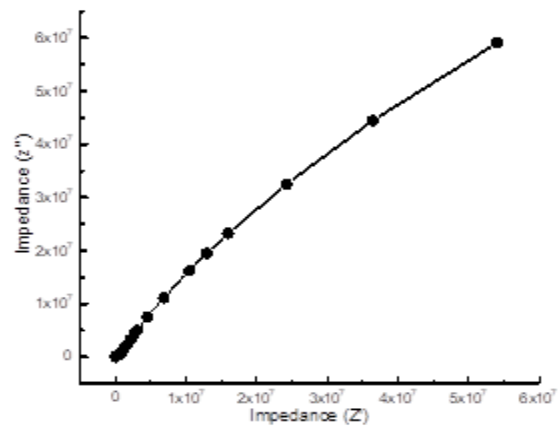


Figure 12: Nyquist's plot of $Ba_{0.9}Ca_{0.1}TiO_3$ perovskite compound

The impedance graph $Ba_{0.9}Ca_{0.1}TiO_3$ sample is displayed in Figure 12. A Nyquist's plot, which plots the imaginary (Z'') versus real (Z') part of the impedance, is referred to as an impedance spectrum. For the $Ba_{0.9}Ca_{0.1}TiO_3$ sample, just one semi-circular arc has been obtained in the sample currently under investigation. The diameter of the semicircle,

however, can be easily extrapolated, indicating that the grain interior is primarily responsible for the impedance. This is because the grain boundary typically exhibits a much higher resistance than the grain interior due to a potential barrier. Moreover, it appears that the center of semicircle lies well below the Z' axis, indicating non-Debye behavior [20, 21].

CONCLUSION

Literature survey has revealed that Ca doped BaTiO₃ is an indispensable material in the applications viz. dielectric filters, antennas, resonators, duplexers and phase shifters, capacitors and piezoelectric actuators. The experimentally prepared Ba_{0.9}Ca_{0.1}TiO₃ perovskite compound has been found single phased crystallized in tetragonal phase inferred from XRD and Rietveld refinement analysis. The dielectric properties are extremely worth mentioning where dielectric permittivity values are relatively large whereas dielectric loss is comparatively low when comparative study is taken into consideration. Impedance analysis further revealed the sample to lose impedance when applied value is applied. Further, the impedance witnesses the distributed time relaxations with the behaviour to be non-Debye type.

ACKNOWLEDGEMENTS

Authors acknowledge the SAGE University as an institute and department of physics sage university and its faculty for constant support. GHS College, Indore (M.P.), department of Physics, Dr. Netram Kaurav (Materials Research Lab, GHS College, Indore (M.P.) are extended warm thanks for extending support

REFERENCES

- [1] W. Liu, X. Ren, Phys. Rev. Lett. 103 (2009) 257602 (1–4).
- [2] Z. Yu, C. Ang, R. Guo, A.S. Bhalla, J. Appl. Phys. 92 (2002) 1489
- [3] Z.Q. Zhuang, M.P. Harmer, D.M. Smyth, R.E. Newnham, Mater. Res. Bull. 22 (1987) 1329.
- [4] A. A. Bokov, Ferroelectrics 131 (1992) 49–55
- [5] C.-X. Lia, B. Yanga, S.-T. Zhang, R. Zhang, W.-W. Cao, Ceram. Int. 39 (2013) 2967–2973.
- [6] M.H. Frey, Z. Xu, P. Han, D.A. Payne, Ferroelectrics 206 (1998) 337–353
- [7] M. H. Khedhri, N. Abdelmoula, H. Khemakhem, R. Douali, F. Dubois, Applied Physics A 125 (2019) 193
- [8] R. Muhammad, M. A. Khalila, M. S. Castro, Ceramics International, Ceramics International, 46 (2020) 1059-1064
- [9] Y. A. Zulueta, M. T. Nguyen, M. P. Pham-Ho, Journal of Physics and Chemistry of Solids 182, (2023) 111564
- [10] V. S. Puli, D. K. Pradhan, B. C. Riggs, D. B. Chrisey, R. S. Katiyar Journal of Alloys and Compounds 584 (2014) 369–373
- [11] M. Sindhu, N. Ahlawat, S. Sanghi, R. Kumari, A. Agarwal, Journal of Applied Physics 114 (2013) 164106.
- [12] A. Salhia, S. Sayouri, A. Alimoussa, L. Kadira, Materials Today: Proceedings 13 (2019) 1248–1258
- [13] M. C. Chang, S. C. Yu, Materials Science Letters 19 (2000) 1323- 1325.
- [14] M. R. Panigrahi, S. Panigrahi, Physica B: Condensed Matter, 405 (2010) 2556-2559
- [15] X. Cheng, M. Shen Materials Research Bulletin, 42 (2007) 1662-1668
- [16] Y. Yang, H. Hao, L. Zhang, C. Chen, Z. Luo, Z. Liu, Z. Yao, M. Cao, H. Liu Ceramics International, 44 (2018) 11109-11115
- [17] C.K. Suman, K. Prasad, R.N.P. Choudhary, J. Mater. Sci. 41 (2006) 369.
- [18] A. K. Jonscher, Nature 267 (1977) 673–679.
- [19] K. Feliksik, L. Kozielski, I. Szafraniak-Wiza, T. Goryczka, and M. Adamczyk-Habrajska Materials (Basel). 12(24) (2019) 4036.
- [20] J. Wu, J. Wang, J. Appl. Phys., 110 (2011), 064104.
- [21] N. Gouitaa, T. Lamcharf, M. Bouayad, F. Abdi, N. Hadi, Journal of Materials Science: Materials in Electronics, 29(8) 2018) 6797–6804